NASA/CR–20250008764

Experimental Mode Orthogonality and its Consequences

Robert N. Coppolino
Measurement Analysis Corporation, Torrance, California

August 2025

NASA STI Program Report Series

Since its founding, NASA has been dedicated to the advancement of aeronautics and space science. The NASA scientific and technical information (STI) program plays a key part in helping NASA maintain this important role.

The NASA STI program operates under the auspices of the Agency Chief Information Officer. It collects, organizes, provides for archiving, and disseminates NASA's STI. The NASA STI program provides access to the NTRS Registered and its public interface, the NASA Technical Reports Server, thus providing one of the largest collections of aeronautical and space science STI in the world. Results are published in both non-NASA channels and by NASA in the NASA STI Report Series, which includes the following report types:

- TECHNICAL PUBLICATION. Reports of completed research or a major significant phase of research that present the results of NASA Programs and include extensive data or theoretical analysis. Includes compilations of significant scientific and technical data and information deemed to be of continuing reference value. NASA counterpart of peer-reviewed formal professional papers but has less stringent limitations on manuscript length and extent of graphic presentations.

- TECHNICAL MEMORANDUM. Scientific and technical findings that are preliminary or of specialized interest, e.g., quick release reports, working papers, and bibliographies that contain minimal annotation. Does not contain extensive analysis.

- CONTRACTOR REPORT. Scientific and technical findings by NASA-sponsored contractors and grantees.

- CONFERENCE PUBLICATION. Collected papers from scientific and technical conferences, symposia, seminars, or other meetings sponsored or co-sponsored by NASA.

- SPECIAL PUBLICATION. Scientific, technical, or historical information from NASA programs, projects, and missions, often concerned with subjects having substantial public interest.

- TECHNICAL TRANSLATION. English-language translations of foreign scientific and technical material pertinent to NASA's mission.

Specialized services also include organizing and publishing research results, distributing specialized research announcements and feeds, providing information desk and personal search support, and enabling data exchange services.

For more information about the NASA STI program, see the following:

- Access the NASA STI program home page at http://www.sti.nasa.gov

- Help desk contact information:

https://www.sti.nasa.gov/sti-contact-form/
and select the "General" help request type.

NASA/TM–20250008764

Experimental Mode Orthogonality and its Consequences

Robert N. Coppolino
Measurement Analysis Corporation, Torrance, California

National Aeronautics and
Space Administration

Langley Research Center
Hampton, Virginia 23681-2199

Prepared for Langley Research Center
under Contract 80LARC23DA003

August 2025

Available from:

NASA STI Program / Mail Stop 050
NASA Langley Research Center
Hampton, VA 23681-2199

Experimental Mode Orthogonality and its Consequences

Robert N. Coppolino
Measurement Analysis Corporation
23850 Madison Street, Torrance CA 90905 USA

Abstract

This document addresses enduring challenges encountered in modern experimental modal analysis as well as earlier "resonance testing" associated with measured mode orthogonality requirements. To this end, the document's goals are (1) retirement of false damping and real mode notions (dating back to Lord Rayleigh, 1877), (2) achievement a community consensus on 85+ years of resonance and modal testing, and (3) establishment of an experimental modal analysis process that is independent of a-priori predictive mathematical models. The above goals are satisfied by addressing six key objectives, namely (a) validation of measured complex experimental modes, (b) empirical isolation of experimental modes (the "Holy Grail" of resonance testing), (c) definition of a state-space orthogonality standard, independent of an approximate reduced-order mass matrix, (d) exploitation of state-space, left-hand eigenvectors and their relationship to modal momentum and kinetic energy distributions, (e) establishment of a universal practice for a broad family of modal testing methods, and (f) application of the above six objectives to ambient (operational modal analysis) methods.

[Orthogonality, State-Space, Modal, Isolation]

Nomenclature

[B]	Damping Matrix
{F}	Applied Load Array
[H]	Frequency Response Matrix
[K]	Stiffness Matrix
[KE]	Modal Kinetic Energy Matrix
[M]	Mass Matrix
[OR]	Orthogonality Matrix
[V]	SVD Trial Vector Matrix
[h]	Generalized Frequency Response Matrix
{q}	Modal Displacement Array
t	Time
{u}	Displacement Array
[z]	SVD Generalized Variable Matrix
$[\ ]^T$	Transpose of a Real or Complex Matrix

[A]	State-Space Plant Matrix
[B]	State-Space Excitation Matrix
[X]	State-Space Response Matrix
$[\Delta]$	Modal Orthogonality"Error" Matrix
$[\Phi]$	Modal Matrix
$[\Gamma]$	Applied Load Allocation Matrix
[I]	Identity (Matrix)
[P]	Modal Momentum Matrix
α	Rayleigh Damping Mass Coefficient
β	Rayleigh Damping Stiffness Coefficient
$[\varphi]$	Modal Matrix Partition
$[\lambda]$	Eigenvalue Matrix
ω	Frequency (radian units)
ζ	Critical Damping Ratio

1.0 Introduction

Modal testing, previously called resonance testing (Gladwell and Bishop)[1] has its origins (most likely) prior to Walker and Clegg's documented wing tests in 1939[2], more than 86 years ago. Gladwell and Bishop's publication offers an extensive commentary and critique of resonance testing strategies, focusing on response to swept and dwell sinusoidal stimuli, up to 1963. The modern digital era of experimental modal analysis [3,4], initiated after 1970, owes much of its foundations on the Cooley and Tukey's FFT algorithm[5] and Bendat and Piersol's random data analysis courses and books[6]. The primary emphasis in resonance testing is experimental isolation of individual "normal" modes, while the prevalent practice in experimental modal analysis is "curve fitting" of complex or real modes to measured frequency response data, especially emphasized in early pioneering work by Richardson and Potter[7], as well as many other authors.

During monthly meetings of The SAE G-5 Committee on Shock and Vibration, at the Aerospace Corporation in the 1970's, the prevailing opinion of aeronautical and aerospace technologists was that experimental modal data needed to be validated (regardless of resonance testing or experimental modal analysis philosophy) by satisfaction of a mass-weighted modal orthogonality standard. Such standards have been codified by NASA[8] and the U.S. Air Force Space Command[9]. The inherent inconsistency associated with mass-weighted model orthogonality standards lies in the implied assumption that measured modes must be <u>real</u>, in spite of strong evidence that they may be <u>complex</u> (to some extent). Commonplace practice at modal testing organizations includes strategies to <u>artificially</u> constrain complex experimental modes to real form.

The present document deliberately side-steps all established mass-weighted orthogonality practices by full acceptance of complex analytical and measured modes, based on the fact that the mathematical construct of proportional damping has never been observed or analytically justified (many references and technical community experiences justifying this position are not specifically cited herein). Three foundational points are emphasized in this document, namely:

1. Complex modes resulting from an empirical state-space model are mathematically orthogonal, based on computed left- and right-hand complex eigenvectors (modes). An explicit mass matrix is not required to mathematically define complex mode orthogonality.

2. Pre-multiplication of measured frequency response functions and/or time history response arrays by left-hand complex eigenvectors produces completely uncoupled "signatures", automatically satisfying the elusive "Holy Grail" of resonance testing.

3. State-space format, complex left-hand eigenvectors may be rigorously constructed from right-hand complex eigenvectors and eigenvalues, deduced via non-state-space experimental modal analysis algorithms. This result opens the previous two benefits to virtually all experimental modal analysis and operational (ambient) modal analysis techniques.

2.0 The False Myth of Real Structural Dynamic Modes, Real Mode Obsessions, and its Undoing

2.1 Real Structural Dynamic Modes

The matrix equation set describing linear, small deformation of a structure subjected to dynamic excitations is,

$$[M]\{\ddot{u}\}+[B]\{\dot{u}\}+[K]\{u\}=[\Gamma_e]\{F_e\}. \tag{1}$$

Finite element structural dynamic modeling[10] is widely employed today to construct theoretical expressions for a particular system's mass and stiffness matrices from which undamped real-valued eigenvalues (modes) and eigenvectors are computed, specifically,

$$[K][\Phi_u]=[M][\Phi_u][\lambda], \tag{2}$$

where after (unit modal mass) normalization,

$$[\Phi_u]^T[M][\Phi_u]=[OR]=[I]\ ,\ [\Phi_u]^T[K][\Phi_u]=[\lambda]=[\omega_n^2]. \tag{3}$$

In addition, rigorous expressions for modal "momentum" and modal "kinetic energy" distributions are defined, respectively, as:

$$[P_{\Phi_u}]=[M][\Phi_U]\ ,\ [KE_{\Phi_u}]=[P_{\Phi_U}]\otimes[\Phi_U]. \tag{4}$$

The sum of modal kinetic energy terms for each normalized mode is always unity.

In 1877, Lord Rayleigh speculated, "The first case occurs frequently, *in books at any rate*, when motion of each part of the system is resisted by a retarding force, proportional both to the mass and velocity of the part. The same exceptional reduction is possible when *F (the dissipation force)* is a linear function of *T (kinetic energy)* and *V (strain energy)*"[11]. That statement forms the basis for the well-known (never empirically demonstrated) "Rayleigh" matrix expression for proportional (viscous) damping,

$$[B_R]=\alpha[M]+\beta[K]. \tag{5}$$

Subsequently Caughey and O'Kelly[12] hypothesized a generalization of proportional damping,

$$[B_C]=[M]\cdot\sum_{n=1}^{N}\left([M]^{-1}[K]\right)^n\ . \tag{6}$$

The ultimate speculative damping matrix, incorporating desired or "somewhat empirical" modal damping coefficients, ζ_n, is of the form

$$[B_U]=[M\Phi][2\zeta_n\omega_n][\Phi^T M]. \tag{7}$$

As a general rule, a structure's theoretical finite element mass and stiffness matrices are "sparse". If damping distribution is modeled in accordance with experimental observations[13] (indicating that a built-up structure's damping is primarily concentrated at joints), the theoretical damping matrix is likewise sparse. Both Caughey-O'Kelly and ultimate speculative damping forms are fully populated, and therefore judged physically implausible.

All three of the above described speculative forms of a theoretical damping matrix continue to be employed in theoretical structural dynamic analyses, since they preserve a convenient (yet false) fact that the damped structure's eigenvectors must be identical to its undamped eigenvectors. Specifically,

$$\left[\Phi_u^T\right]\left[B_R\right]\left[\Phi_u\right],\ \left[\Phi_u^T\right]\left[B_C\right]\left[\Phi_u\right],\ \left[\Phi_u^T\right]\left[B_U\right]\left[\Phi_u\right] = \text{diagonal matrices.} \tag{8}$$

The logical outcome of the above described "false myth of real structural dynamic modes" is the arguably blind condition that has strongly influenced the field of modal testing is "real mode obsessions".

2.2 Complex Structural Dynamic Modes

Hypothesizing a more general damping model (that may be of symmetric or non-symmetric form), a subject structural model's eigenvectors are most likely complex (sometimes or often "approximately" real). Determination of the complex eigenvalues and eigenvectors of such a model is accomplished by solution of state-space equation set of the form,

$$\begin{Bmatrix} \ddot{u} \\ \dot{u} \end{Bmatrix} = \begin{bmatrix} -M^{-1}B & -M^{-1}K \\ I & 0 \end{bmatrix} \begin{Bmatrix} \dot{u} \\ \dot{u} \end{Bmatrix} + \begin{bmatrix} M^{-1}\Gamma_e \\ 0 \end{bmatrix} \{F_e\}. \tag{9}$$

The above equation set conforms to the "first-order" algebraic eigenvalue problem[5],

$$\{X\} = \begin{Bmatrix} \dot{u} \\ u \end{Bmatrix},\ \{\dot{X}\} = [A]\{X\} + [B]\{F_e\}. \tag{10}$$

The state-space, complex eigenvalues and eigenvectors for the above damped system are solutions of the algebraic eigenvalue problem,

$$[A][\Phi] = [\Phi][\lambda], \tag{11}$$

where,

$$[\Phi] = \text{right-hand, complex eigenvectors,}$$

$$\lambda_n = \sigma_n + i\omega_n = \text{complex eigenvectors } (\sigma_n = -\zeta_n\omega_n). \tag{12}$$

The left-hand, complex eigenvectors (for the full set of eigenvectors) are defined as,

$$[\Phi_L] = [\Phi]^{-1}. \tag{13}$$

Solution for an incomplete set of complex eigenvalues and eigenvectors is thoroughly documented by Wilkinson[14].

The following properties of the state-space model solution are most significant for the remaining entirety of this document:

$$[OR] = [\Phi_L][\Phi] \equiv [I],\ [\Phi_L][A][\Phi] \equiv [\lambda] \qquad \text{(orthogonality)} \tag{14}$$

$$\{X\} = [\Phi]\{q\} \qquad \text{(modal transformation)} \tag{15}$$

$$\{\dot{q}\} = [\lambda]\{q\} + [\Phi_L B]\{F_e\} \qquad \text{(uncoupled dynamic equations)} \tag{16}$$

Upon partitioning the state-space right-hand and left-hand complex eigenvectors into “velocity” and “displacement” components, as follows:

$$[\Phi] = \begin{bmatrix} \Phi_V \\ \Phi_U \end{bmatrix},\ [\Phi_L] = [\Phi_{VL} \quad \Phi_{UL}], \tag{17}$$

complex modal “momentum” and modal “kinetic energy” distributions are defined, respectively, as:

$$[P_{\Phi V}] = [\Phi_{VL}]^T \equiv [M][\Phi_V],\ [KE_{\Phi V}] = [P_{\Phi V}] \otimes [\Phi_V] \equiv [M\Phi_V] \otimes [\Phi_V]. \tag{18}$$

It is significant to note that the undamped modal “momentum” and modal “kinetic” energies defined in Section 2.1 are directly proportional to the above corresponding forms when the damping matrix is null. Furthermore, analytical studies that are beyond the scope of this document reveal interesting correspondences and contrasts between undamped, real mode based and complex, state-space based modal “momentum” and modal “kinetic” energy distributions.

2.3 Adjustment of Complex Measured Modes to Real Form

A common practice in U.S. aerospace-oriented laboratories and organizations involves adjustment of complex measured modes (regardless of resonance or digital era experimental modal analysis sources) to approximate real form. Enforcement of each complex mode to an approximate real form generally involves (1) rotation of each estimated complex mode, described in the complex plane, such that its mean DOF component value is on the real axis, followed by (2) accepting the resulting real components produce the desired real mode. The steps in this process are illustrated below in Figure 1 for a hypothetical “slightly” complex experimental mode.

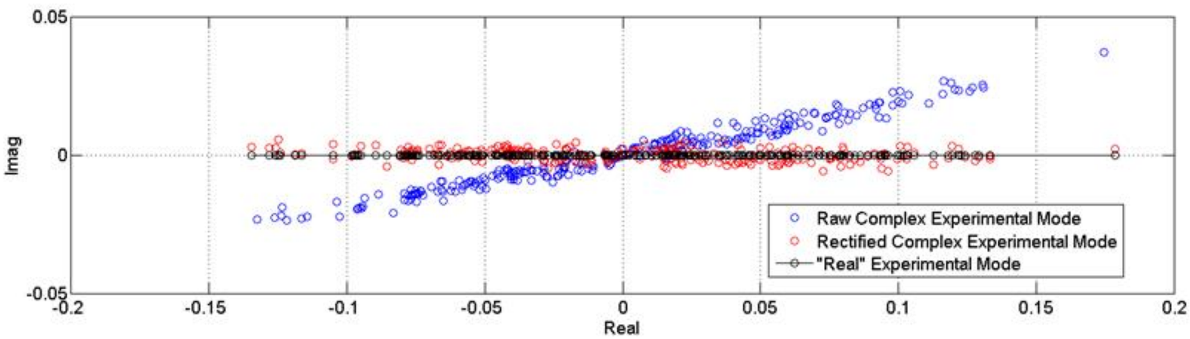

Figure 1: Hypothetical Complex Experimental Mode “Adjustment” to Real Form

Justification for the above process is severely weakened when measured modes of a more “complex” nature occur, especially in situations involving closely-spaced modes.

2.4 Real Mode Orthogonality Criteria

Due to the fact that (multi-shaker, sine-dwell) modes associated with resonance testing are generally recorded within selected sub-bands of the overall frequency band of interest, real mode orthogonality criteria were developed in order to realize (reasonably) orthogonal experimental modes over the entire frequency band of interest. The real modes associated with a theoretical (FEM) model, after unit-mass normalization, are perfectly orthogonal with respect to the FEM mass matrix, [M], i.e.,

$$[\Phi^T M \Phi] = [I]. \tag{19}$$

However, in the case of a resonance or "EMA" modal test, the measured response DOF set is generally much smaller than the FEM DOF set. Therefore, systematic procedures for appropriate selection of the measured response DOF "modal" set, $\left[\Phi_{TAM}\right]$, and reduced-order mass matrix, $\left[M_{TAM}\right]$, have been developed and widely applied. Since the measured modes (as well as the "TAM" partition of FEM modes) do not strictly satisfy mass-weighed orthogonality, normalized, $\left[\Phi_{TAM}\right]$, orthogonality is of the form,

$$\left[\Phi_{TAM}^{T}\right]\left[M_{TAM}\right]\left[\Phi_{TAM}\right] = \left[I\right] + \left[\Delta\right], \tag{20}$$

where $[\Delta]$ is a symmetric matrix with "null" on-diagonal terms.

3.0 Departure from Established U.S. Aerospace Community Practice, A New Way

3.1 The Integrated Test Analysis Process for Structural Dynamic Systems

Over the past 60 years, the U.S. aerospace community has developed, refined and standardized an integrated approach to structural dynamic model verification and validation. One name for this overall approach is the Integrated Test Analysis Process (ITAP)[15] for structural dynamic systems, which is summarized below in Figure 2.

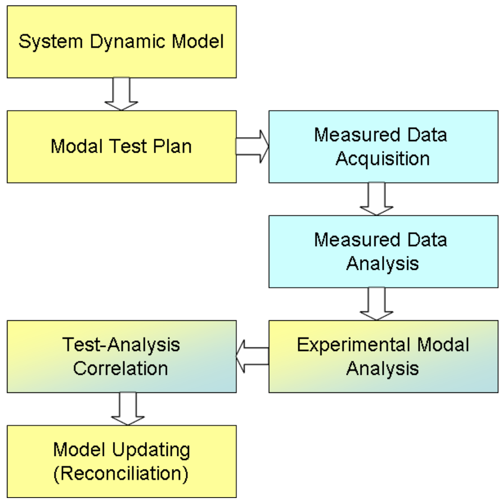

Figure 2: Overview of the Integrated Test Analysis Process

The yellow colored steps are associated with analytical-centric disciplines, while the aqua colored steps are associated with laboratory-centric disciplines. The mixed colored steps involve a blend of analytical and laboratory disciplines. Each step in the process is the product of a variety of authoritative, widely recognized sources.

Experimental modal analysis strategies encompass a broad range of techniques developed during the resonance testing (1939-) and modal testing (1970-) eras. Outlined below in Figure 3, are three general EMA approaches.

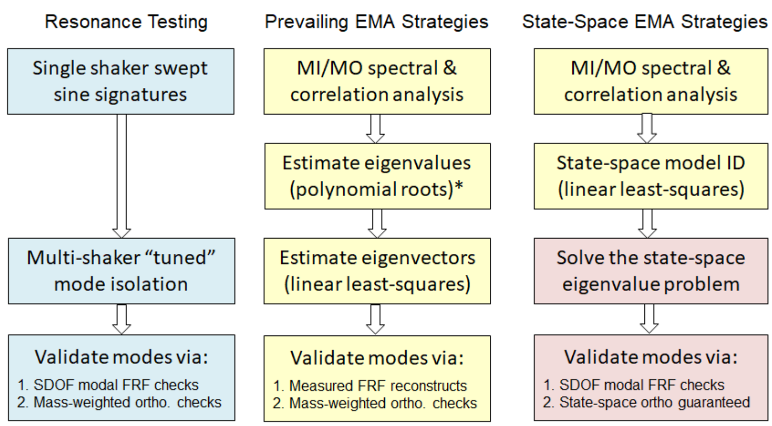

*Classic SFD (1979-1018) employs band limited state-space analysis to estimate eigenvalues

Figure 3: Overview of General EMA Strategies

Resonance Testing was the predominant aerospace community EMA practice prior to 1970, which relied heavily on analog technology. Today, its digital era based implementations (commonly called "force appropriation testing) are employed by a minority of EMA practitioners in the aerospace community.

Validation of experimental modal data associated with Resonance Testing includes (a) empirical (graphical) verification of modal SDOF behavior, and (b) mass-weighted modal orthogonality checks following U.S. government standards.

The Prevailing EMA strategy group, across all technical communities, is characterized by a two-step experimental modal analysis process, which first estimates eigenvalues (modal frequencies and damping coefficients) via solution of polynomial expressions, followed by a separate distinct linear least squares analysis process that estimates the associated complex eigenvectors (modes) of a subject test article. It is of interest to note that prior to 2018, the Classic SFD technique[16,17] employed a two-step process that is similar to the Prevailing EMA strategy group. Specifically, Classic SFD employs state-space estimation to estimate eigenvalues, as its first step, followed by a least-squares process to (a) estimate enforced real eigenvectors or (b) estimate complex eigenvectors. Validation of experimental modal data associated with Resonance Testing includes (a) analytical reconstruction of MI/MO based FRFs based on estimated modal parameters, and (b) mass-weighted modal orthogonality checks following U.S. government standards.

The State-Space EMA strategy group encompasses procedures categorized by Allemang and Brown[3,4] as “low-order models” that operate on both the time- and frequency-domain measured data; to be sure, their categorizations encompass a much broader class of techniques that include ambient/operational modal analysis[18]. The narrower context of State-Space EMA, summarized in Figure 2 is limited to frequency domain techniques with a primary focus on SFD-2018[15]. While this group of techniques employs a MI/MO deduced set of frequency response functions as its starting point, experimental modal analysis follows a two-step process involving (a) state-space model estimation over the frequency band of interest, followed by (b) computation of complex eigenvalues and eigenvectors (modes) by solution of the state-space eigenvalue problem. The final verification step includes quality checks that eliminate spurious modes and acceptance of mathematically perfect state-space orthogonality of the (judged valid) complex experimental eigenvectors (modes). This unique feature of State-Space EMA sets it apart from the other two EMA categories since (1) mass-weighted orthogonality criteria and (2) a-priori mathematical model data are totally irrelevant to the process. In short, State-Space EMA represents a radical departure from all previous experimental modal estimation schemes.

3.2 Why Departure from Mass-Weighted Orthogonality Criteria is Necessary

Independent analysis of time history data from NASA’s ISPE Upper Stage modal test (Marshall Space Flight Center, 2016), employing Classic SFD (part of the Prevailing EMA strategy group), revealed a seriously deficient mass-weighted orthogonality check[8] as noted below in Figure 4.

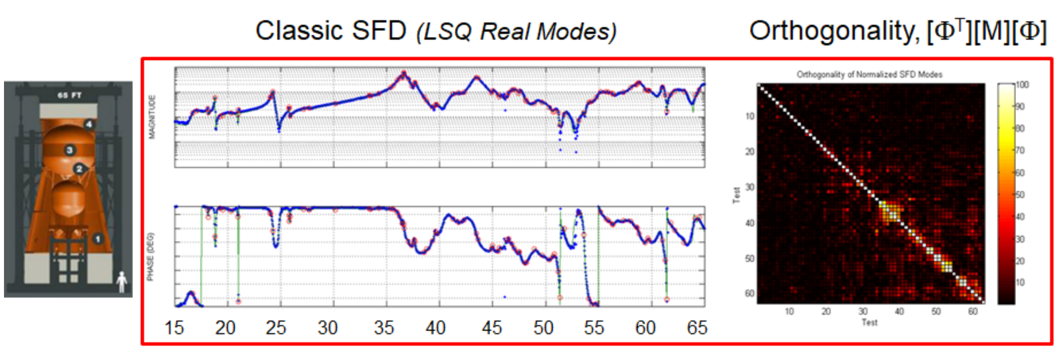

Figure 4: Overview of ISPE Upper Stage Modal Test Data

The EMA process employed included a much used Classic SFD option that directly computed real experimental modes (no adjustment of complex experimental modes was required). Reconstruction of high quality MI/MO based FRFs employing the estimated modal data proved quite remarkable, as indicated in the magnitude and phase FRF display. However, the modal orthogonality check revealed significant violations of NASA’s mass-weighted orthogonality standard (≤ 10% off-diagonal coupling terms). The ISPE experience necessitated more aggressive rethinking of the Classic SFD technique, which previously showed a great deal of success in prior modal testing projects.

3.3 SFD-2018 A Radical Departure from Established Conventions

Rethinking of the Simultaneous Frequency Domain (SFD) technique ultimately led to the introduction of SFD-2018, which has been thoroughly documented[15]. A general overview of SFD-2018 is summarized below in Figure 5.

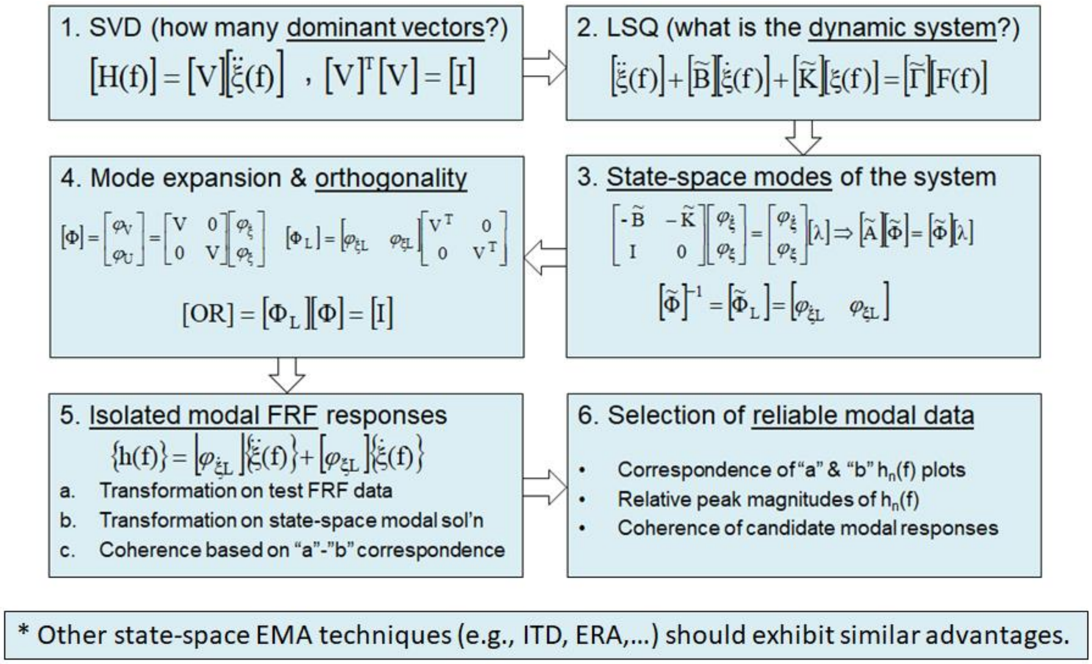

Figure 5: Overview of the SFD-2018 Process

Steps 1-3 in the SFD-2018 process are mathematically the same as implemented in Classic SFD, with the following innovations:

1. The tolerance coefficient employed in singular value decomposition (SVD) is a deliberately small number (originally a fixed value ε = .01 default, now typically $\varepsilon \leq 10^{-4}$) in order to capture details within one broad frequency band, rather than selected narrow sub-bands, in order to define fully encompassing dominant SVD vectors, [V], and associated generalized accelerations, $\ddot{\xi}(f)$.
2. Least squares estimation of effective dynamic system matrices over a single broad band.
3. Broad band state-space eigenvalue solution, including left-hand eigenvectors, in terms of reduced generalized coordinates, $\xi(f)$.

Continuing additional steps include:

4. The generalized complex left- and right-hand eigenvectors are expanded to response coordinate order, H(f), using the reduced set of real orthogonal vectors, V. State-space orthogonality is perfectly satisfied by the mathematical process, eliminating the need for a mass-weighted orthogonality standard and rendering EMA validation totally independent of a theoretical mathematical model.
5. Computation of generalized modal FRFs re-introduces a feature of Resonance Testing that validated experimental mode isolation based on observed single degree-of-freedom modal response qualities.
6. Quantitative review of all mathematically calculated modal FRFs permits selection of a subset of estimated complex eigenvectors (modes) and rejection of extraneous "noise" modes.

A brief overview of SFD-2018 ISPE experimental modal analysis results, specifically related to modal isolation, is provided below in Figure 6.

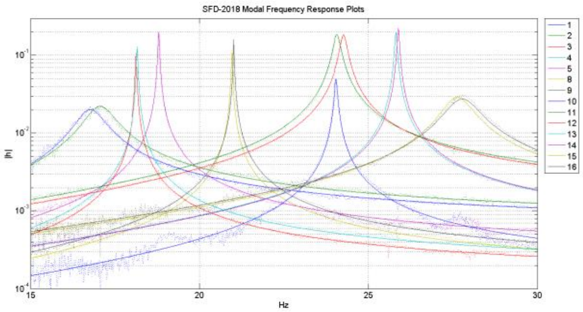

EV Attributes				|h| (%)				|coh| (%)			
Mode	Freq (Hz)	Zeta (%)	Index (%)	1	2	3	4	1	2	3	4
1	16.761	2.399	0.1	2.69	2.07	1.52	0.65	99	99	98	88
2	17.048	2.445	0.3	0.83	1.81	2.54	2.76	88	98	99	99
3	18.124	0.096	0.1	3.65	2.11	3.57	10.78	82	75	43	99
4	18.161	0.098	0.7	15.11	6.55	4.43	3.11	99	78	72	73
5	18.792	0.102	0.0	23.57	26.24	21.92	23.91	98	92	98	99
6	20.025	3.296	10.5	0.95	0.42	1.27	0.90	91	50	93	93
7	20.316	2.344	0.7	1.13	0.74	1.06	0.43	98	96	97	94
8	20.955	0.086	0.0	7.46	11.57	14.56	7.86	97	95	98	96
9	21.012	0.075	0.0	19.24	12.16	16.37	11.06	99	94	95	95
10	24.041	0.178	11.1	3.37	1.42	1.91	5.45	98	93	94	99
11	24.068	0.452	0.2	1.63	14.02	13.82	22.48	71	100	100	100
12	24.266	0.414	0.3	21.04	14.38	16.75	1.13	100	100	100	41
13	25.818	0.129	0.0	23.39	10.33	8.73	7.18	100	98	98	93
14	25.888	0.114	0.0	5.76	10.66	12.19	24.75	84	89	91	99
15	27.630	1.497	6.6	3.51	1.07	1.67	3.67	100	93	91	100
16	27.774	1.679	7.8	1.12	3.69	3.80	1.35	94	99	99	95
17	30.150	0.128	0.0	10.58	7.13	5.69	9.41	99	95	90	99

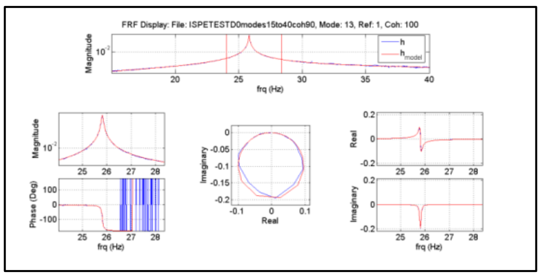

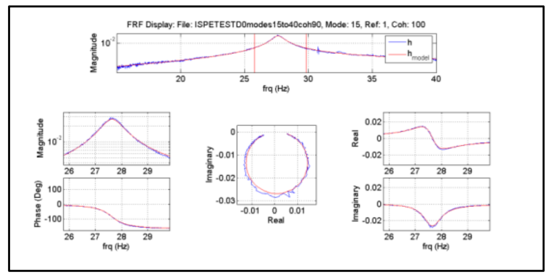

Figure 6: SFD-2018 Modal Isolation for the ISPE Modal Test (2016)

The upper left plot displays “SDOF” $h_n(f)$ amplitude vs. frequency associated with SFD-2018 estimated modes 1-5 and 8-17. On the upper right is a summary table listing modal attributes (blue indicating approximately real modes with complex index <1, yellow indicating clearly complex modes with complex index >1, and grey indicating poorly excited modes, 6 & 7, low overall amplitude and “modal” coherence). The lower left and right displays are detailed (selected sub-band magnitude, magnitude and phase, polar, real and imaginary) $h_n(f)$ plots associated with predominantly real mode 13, and complex mode 15, respectively.

3.4 Experimental Mode Orthogonality and Individual Modal Isolation for all EMA Techniques

SFD-2018 introduced two interrelated benefits that satisfied the aspirations of Experimental Modal Analysis and Resonance Testing, namely:

1. Satisfaction of experimental modal orthogonality standards[8,9] independent of a theoretical TAM mass matrix.
2. Isolation of individual experimental modes without applied force tuning[1] (modal force appropriation).

These benefits may be realized by all EMA techniques based on straightforward mathematical constructs that operate on the basic (frequency domain) EMA products, namely:

(a) Measured frequency response matrices, $[H_1(f)]$, $[H_2(f)]$,…,$[H_N(f)]$, 1,2,…N are excitation indices.

(b) Empirical eigenvectors (complex modes), $[\varphi_v]$ (related to response motions, not state-space).

(c) Empirical eigenvalues, $\lambda_n = -\zeta_n \cdot \omega_n + i \cdot \omega_n$ (only positive-valued frequencies).

(d) Measured time history responses, $[\ddot{U}(t)]$ (primarily for ambient/operational modal analysis).

State-space eigenvectors are mathematically defined by appending acceleration and constructed velocity components as follows:

$$[\Phi] = \begin{bmatrix} \varphi_V \\ \varphi_U \end{bmatrix} = \begin{bmatrix} \varphi_V \\ \varphi_V \cdot \lambda_n^{-1} \end{bmatrix}. \tag{21}$$

The left-hand eigenvectors are constructed employing a two-step process as follows:

Step 1 (SVD): $[\varphi_V] = [V][z] \ldots [V^T][V] = [I]$ and $[z]$ is square and non-singular. (22)

Step 2 (Construction): $[\Phi_L] = [\varphi_{VL} \quad \varphi_{UL}] = \left(\dfrac{1}{2}\right) \cdot [z^{-1} \cdot V^T \quad \lambda_n \cdot z^{-1} \cdot V^T]$ (23)

It is clear that the product of left- and right-hand eigenvectors produces “perfect” state-space orthogonality, i.e.,

$$[OR] = [\Phi_L] \cdot [\Phi] = [\varphi_{VL} \quad \varphi_{UL}] \cdot \begin{bmatrix} \varphi_V \\ \varphi_U \end{bmatrix} = \left(\frac{1}{2}\right) \cdot [z^{-1} \cdot V^T \quad \lambda_n \cdot z^{-1} \cdot V^T] \cdot \begin{bmatrix} V \cdot z \\ V \cdot z \cdot \lambda^{-1} \end{bmatrix} \equiv [I]. \tag{24}$$

It is important to note that there is a subtle difference between left-hand eigenvectors associated with SFD-2018 and those estimated by the above recipe for all EMA techniques (which in actuality falls in the broad category of pseudo-inverse strategies).

State-space form measured frequency response functions are constructed as follows:

$$[H_{SS,K}(f)] = \begin{bmatrix} H_K(f) \\ H_K(f) \cdot \mathrm{diag}[2\pi f]^{-1} \end{bmatrix}. \tag{25}$$

The “modal” generalized frequency response functions, readily calculated as the products associated with each excitation index,

$$[h_{SS,K}(f)] = [\Phi_L] \cdot [H_{SS,K}(f)]. \tag{26}$$

Note that the above described process permits SFD-2018 (Steps 4 and 5) modal orthogonality and modal isolation benefits (outlined in Figure 5) for “all frequency domain EMA” techniques, as demonstrated by a comparison of ISPE test related SFD-2018 and $[h_{SS,K}(f)]$ magnitude versus frequency functions (for ISPE modes 1-5 and 8-17, ignoring “poor” quality modes 6-7) below in Figure 7.

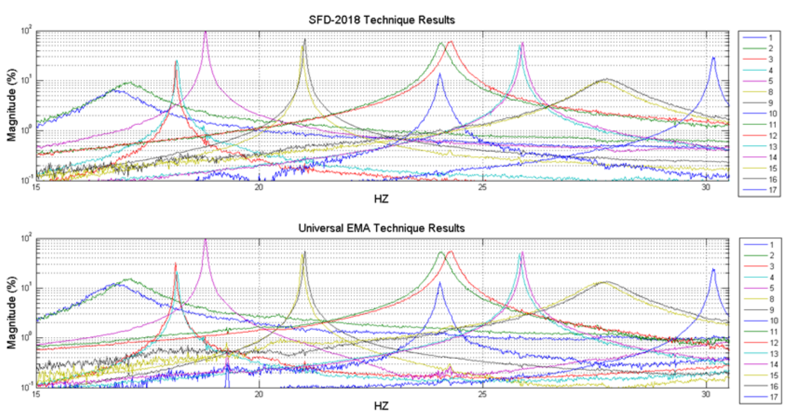

Figure 7: SFD-2018 and “Universal EMA” Modal Isolation for the ISPE Modal Test (2016)

Regarding the issue of EMA mass-weighted orthogonality, the following cases were examined:

a. $[OR]=[\varphi_V]^H[M_{AA}][\varphi_V]$, $[\varphi_{VL}]=[\varphi_V]^H[M_{AA}]$ for complex non-state-space EMA modes

b. $[OR]=[real(\varphi_V)]^T[M_{AA}][real(\varphi_V)]$, $[\varphi_{VL}]=[real(\varphi_V)]^T[M_{AA}]$ for non-state-space, real EMA modes

c. $[OR]=[\Phi_L][\Phi]\equiv[I]$ for state-space EMA or SFD-2018 modes.

Results of the above three cases for ISPE modes 1-17 are summarized below in Figure 8.

Mode	1	2	3	4	5	6	7	8	9	10	11	12	13	14	15	16	17
Freq (Hz)	16.76	17.05	18.12	18.16	18.79	20.03	20.32	20.95	21.01	24.04	24.07	24.27	25.82	25.89	27.63	27.77	30.15
Zeta (%)	2.399	2.445	0.096	0.098	0.102	3.296	2.344	0.086	0.075	0.178	0.452	0.414	0.129	0.114	1.497	1.679	0.128
Index (%)	0.12	0.34	0.10	0.66	0.03	10.53	0.67	0.03	0.02	11.10	0.25	0.33	0.05	0.03	6.60	7.80	0.02
$[OR]=[\Phi_V]^T[M_{TAM}][\Phi_V]$ (abs %)	100	7	1	4	3	11	3	1	2	10	2	4	4	2	4	4	1
	7	100	9	5	6	7	12	1	2	8	1	3	1	4	8	4	2
	1	9	100	9	1	2	2	1	6	3	6	3	3	1	1	2	2
	4	5	9	100	3	1	1	5	2	1	2	4	2	9	2	1	5
	3	6	1	3	100	3	1	1	4	1	2	6	0	6	0	2	3
	11	7	2	1	3	100	68	1	1	11	20	3	1	3	9	13	1
	3	12	2	1	1	68	100	2	1	7	11	5	1	2	7	2	0
	1	1	1	5	1	1	2	100	3	2	3	2	2	0	2	0	3
	2	2	6	2	4	1	1	3	100	1	1	3	2	1	1	1	1
	10	8	3	1	1	11	7	2	1	100	54	6	1	1	17	7	2
	2	1	6	2	2	20	11	3	1	54	100	5	2	3	2	2	5
	4	3	3	4	6	3	5	2	3	6	5	100	3	7	1	2	3
	4	1	3	2	0	1	1	2	2	1	2	3	100	1	1	2	4
	2	4	1	9	6	3	2	0	1	1	3	7	1	100	1	0	5
	4	8	1	2	0	9	7	2	1	17	2	1	1	1	100	55	2
	4	4	2	1	2	13	2	0	1	7	2	2	2	0	55	100	2
	1	2	2	5	3	1	0	3	1	2	5	3	4	5	2	2	100
$[OR]=[real(\Phi_V)]^T[M_{TAM}][real(\Phi_V)]$, (abs %)	100	5	0	2	3	11		1	2	11	2	4	4	2	4	4	1
	5	100	6	3	5	7	12	1	2	9	1	3	1	4	8	4	1
	0	6	100	5	1	2	2	1	6	3	6	3	3	1	0	2	2
	2	3	5	100	3	1	0	5	2	1	2	4	2	9	2	0	5
	3	5	1	3	100	3	1	1	4	1	2	6	0	6	0	2	3
	11	7	2	1	3	100	66	0	0	8	19	3	1	3	5	11	1
	2	12	2	0	1	66	100	0	1	4	10	5	1	2	7	1	0
	1	1	1	5	1	0	0	100	3	1	3	2	2	0	2	0	3
	2	2	6	2	4	0	1	3	100	0	1	3	2	1	1	1	1
	11	9	3	1	1	8	4	1	0	100	28	0	0	0	20	9	1
	2	1	6	2	2	19	10	3	1	28	100	5	2	1	1	1	5
	4	3	3	4	6	3	5	2	3	0	5	100	1	7	1	1	3
	4	1	3	2	0	1	1	2	2	0	2	1	100	1	0	2	4
	2	4	1	9	6	3	2	0	1	0	1	7	1	100	1	0	5
	4	8	0	2	0	5	7	2	1	20	1	1	0	1	100	30	2
	4	4	2	0	2	11	1	0	1	9	1	1	2	0	30	100	2
	1	1	2	5	3	1	0	3	1	1	5	3	4	5	2	2	100
$[OR]=[\Phi_L][\Phi]$, (abs %)	100																
		100															
			100														
				100													
					100												
						100											
							100										
								100									
									100								
										100							
											100						
												100					
													100				
														100			
															100		
																100	
																	100

Figure 8: Overview of Three ISPE Modal Orthogonality Cases (absolute values of [OR])

It is of particular interest to review the performance of cases "a" and "b" (application of the real part of complex experimental modes) as attempts to isolate modal FRF behavior. Results associated with ISPE mode 10, detailed in Figure 9 below, indicate failure of artificial enforcement of real mode behavior to effect experimental mode isolation.

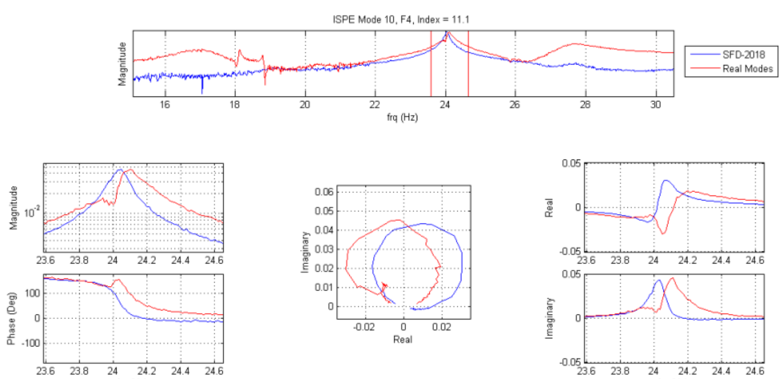

Figure 9: Attempts to Demonstrate Mode Isolation Employing Non-state-space Left-Hand Eigenvectors

The following observations are made regarding the above three cases:

Case 1: Modal orthogonality does not satisfy U.S. government criteria for modes with Index > 10% (shaded yellow)

Case 2: Modal orthogonality improves somewhat when real parts of complex modes are employed

Case 3: State-space modal orthogonality is mathematically perfect for “Universal EMA” complex modes.

It is clear that <u>Experimental Mode Orthogonality and Individual Modal Isolation for all EMA Techniques</u> demonstrate:

1. Effective modal isolation (which <u>Resonance Testing</u> has <u>never</u> completely satisfied) without the need for laborious excitation tuning (force appropriation).
2. Validation of complex modes via the left-hand eigenvector FRF transformation, while employment of constrained real left-hand eigenvector FRF transformation fails to do likewise.
3. Perfect satisfaction of modal orthogonality without the need for a TAM mass matrix.
4. Complete separation of the EMA process from mathematical model predictions.

3.5 Modal Orthogonality and Individual Modal Isolation for Time Domain EMA Techniques

The above benefits demonstrated for frequency domain EMA techniques carry over to time domain EMA techniques, including Ambient and Operational Modal Analysis techniques that do not necessarily require known excitation sources. Ambient measurement and analysis situations operate on a time history array, $[\ddot{U}(t)]$, for which the rows are associated with individual channel accelerations. The ultimate results of such time domain EMA techniques are complex eigenvalues and eigenvectors, which conform to all of the orthogonality related results described in section 3.4 of this document. However, modal isolation associated with measured frequency responses must be replaced with time domain considerations that are described below:

Step 1: Employ band-pass filtering and numerical integration to form the state-space time history array,

$$[\dot{X}(t)] = \begin{bmatrix} \ddot{u}(t) \\ \dot{u}(t) \end{bmatrix}. \qquad (27)$$

Step 2: Apply the left-hand eigenvector transformation (employing its complex conjugate transformation, as well) to form the real state-space time history array, to form the real “modal” array,

$$[\dot{q}(t)] = [\Phi_L]\cdot[\dot{X}(t)] + \mathrm{conj}([\Phi_L])\cdot[\dot{X}(t)]. \qquad (28)$$

Step 3: Compute (a) power spectra associated with each of the individual real “modal” array component and (b) perform selected signal processing operations (in this discussion, randomdec signature operations[15] were found to be a useful demonstration tool) to verify single degree-of freedom behaviors.

Results of this exercise on ISPE acceleration response time history data (modal power spectra and mode 10 randomdec signature FFT analyses) are summarized below in Figure 10.

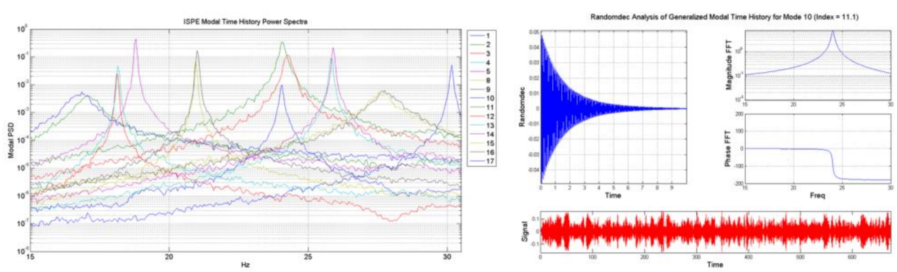

Figure 10: ISPE Power Spectra for Modal Time Histories and Mode 10 Randomdec Analysis

4.0 Conclusions

The primary source of difficulties experienced in Resonance Testing (1939-present) and Modal Testing (1970-present) is Lord Rayleigh's 1877 speculative proportional damping hypothesis, which implies that a structure's modes must be real. An overwhelming body of empirical data indicates that proportional damping is a false hypothesis. Moreover, both theoretical mathematical analyses and modern modal testing technology clearly indicate the "actuality" of complex modes (which are often approximately real nevertheless).

This document offers a viable alternative to challenging practices employed in Resonance Testing and Modal Testing based on three foundational points, namely:

1. Complex modes resulting from an empirical state-space model are mathematically orthogonal, based on computed left- and right-hand complex eigenvectors (modes). An explicit mass matrix is not required to mathematically define complex mode orthogonality.

2. Pre-multiplication of measured frequency response functions and/or time history response arrays by left-hand complex eigenvectors produces completely uncoupled "signatures", automatically satisfying the elusive "Holy Grail" of resonance testing.

3. State-space format, complex left-hand eigenvectors may be rigorously constructed from right-hand complex eigenvectors and eigenvalues, deduced via non-state-space experimental modal analysis algorithms. This result opens the previous two benefits to virtually all experimental modal analysis and operational (ambient) modal analysis techniques.

The findings detailed in this document are intended to specifically address improvements in experimental modal test process. No changes related to (a) test-analysis correlation and reconciliation and (b) the overall load cycle process following U.S. government and other organizational standards are implied or suggested in this work.

The real challenge facing the U.S. Aerospace community, as well as the broader technical community, involves overcoming the "inertia" of long established technical positions and standards that assume/insist "actuality" of mathematically real experimental modes. Once this issue is settled, much broader challenges associated with establishment of procedures and standards dealing with strongly nonlinear-hysteretic structures await the technical community.

References

1. "An Investigation into the Theory of Resonance Testing", R. Bishop and G. Gladwell, Philosophical Trans. of the Royal Society of London, Vol. 255 A 1055, 1963
2. "The Technique of Wing Resonance Tests", P. Walker, P. and A. Clegg, Report No. A. D. 3105/M. T. 11767, Royal Aircraft Establishment, South Farnborough, England, Feb. 1939
3. Harris' Shock and Vibration Handbook, 6th Ed., A. Piersol and T. Paez, McGraw-Hill, 2010, [Chapter 27, Experimental Modal Analysis by R. Allemang and D. Brown]
4. Handbook of Experimental Structural Dynamics, R. Allemang and P. Avitabile, Springer, 2022
5. "An algorithm for the machine calculation of complex Fourier series", J. Cooley and J. Tukey, Mathematics of Computation, 19 (90), 1965.
6. Random Data: Analysis and Measurement Procedures, 4th Ed., J. Bendat and A. Piersol, Wiley, 2010.
7. "Identification of the Modal Properties of an Elastic Structure from Measured Transfer Function Data", M. Richardson and R. Potter, Instrument Society of America, ISA ASI 74250, 1974.
8. "Loads Analysis of Spacecraft and Payloads", Office of the NASA Chief Engineer, NASA Standard 5002A, 2019
9. "Independent Structural Loads Analysis", U.S. Air Force Space Command, SMC-S-004, 2008
10. Fundamentals of Structural Dynamics, 2nd Ed, R. Craig and A. Kurdila, Wiley, 2006
11. The Theory of Sound, Vol. 1, Lord Rayleigh, Cambridge University Press, 2011 (original publication, 1877)
12. "Classical Normal Modes in Damped Linear Dynamic Systems", T. Caughey, and M. O'Kelly, Journal of Applied Mechanics, Vol. 32, 1965
13. Structure Borne Sound, L. Cremer, M. Heckl, and E. Ungar, Springer-Verlag, 1973
14. The Algebraic Eigenvalue Problem, J. Wilkinson, Clarendon Press, 1965
15. The Integrated Test Analysis Process for Structural Dynamic Systems, R. Coppolino, Morgan & Claypool Publishers, 2020
16. "A Simultaneous Frequency Domain Technique for Estimation of Modal Parameters from Measured Data", R. Coppolino, SAE Paper 811046, 1981
17. "A Global Technique for Estimation of Modal Parameters from Measured Data", R. Coppolino and R. Stroud, SAE Paper 851926, 1985
18. Introduction to Operational Modal Analysis, R. Brincker and C. Ventura, Wiley, 2015